Towards understanding the thermoanalysis of water sorption on lithium orthosilicate (Li₄SiO₄)

J. Ortiz-Landeros [a,b], L. Martínez-dlCruz [a], C. Gómez-Yáñez [b], H. Pfeiffer [a,*]

[a] Instituto de Investigaciones en Materiales, Universidad Nacional Autónoma de México, Circuito exterior s/n, Ciudad Universitaria, CP 04510, Del. Coyoacán, México DF, Mexico
[b] Departamento de Ingeniería en Metalurgia y Materiales, ESIQIE, Instituto Politécnico Nacional, UPALM, Av. Instituto Politécnico Nacional s/n, CP 07738, México DF, Mexico

ARTICLE INFO

ABSTRACT

A systematic thermogravimetric study of hygroscopic and reactivity behaviors, at low temperatures of lithium orthosilicate (Li_4SiO_4), are presented. Li_4SiO_4 sample was prepared by solid-state reaction and then treated at different temperature-humidity conditions. Li_4SiO_4 samples previously treated under different temperature-humidity conditions were characterized by Fourier transform infrared spectroscopy and thermogravimetric analyses. Different processes, adsorption and absorption, take place between the Li_4SiO_4 and water vapor. Absorbed water produces superficial hydroxylated species such as Si–OH and Li–OH. In addition, a kinetic analysis was performed, and the different water absorption activation enthalpies were calculated. It was found that activation enthalpy ($\Delta H^{\ddagger}$) values decrease when the relative humidity is incremented, from 5528.6 J/mol to 2074.2 J/mol at relative humidity levels of 60% and 75% respectively. These results show the impact of different humidity and temperature conditions on the stability and/or chemical reactivity of Li_4SiO_4, if this ceramic is used in different application fields, such as carbon dioxide captor or as a breeder ceramic into the fusion reactors.

© 2011 Elsevier B.V. All rights reserved.

1. Introduction

Lithium orthosilicate (Li_4SiO_4) has been widely studied as tritium breeding-material for blankets in nuclear fusion reactors [1–5] and, in more recent years, as a promising carbon dioxide (CO_2) absorbent [6–9]. In these technological applications, as well as in others, the exposition of Li_4SiO_4 to water vapor may affect its performance. In fact, the hygroscopic nature of lithium ceramics is a critical factor in the materials selection for the design of ceramics breeders, due to their moisture affinity, which can produce a decrement in its properties due to the presence of sorbed water [10].

The process of CO_2 capture, using Li_4SiO_4 as a solid absorbent, takes place according to the next reaction:

$$Li_4SiO_{4(s)} + CO_{2(g)} \leftrightarrow Li_2CO_{3(s)} + Li_2SiO_{3(s)} \tag{1}$$
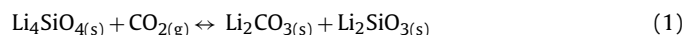
In this case, since water vapor is present as a combustion product, then the solid absorbents are exposed to wet environments especially when post-combustion capture technologies are used [11]. In this sense, some researchers have shown that exposure of solids absorbents to wet environments can affect the CO_2 sorp-

tion performance. For example, Essaky et al. reported the influence of both, low and high humidity conditions, on CO_2 absorption efficiency of Li_4SiO_4 at room temperature [12]. In their work, the authors proposed a model for the reaction including intermediate acid–base reactions with hydrolysis. It was concluded that under dry conditions, once the lithium carbonate is formed as a layer on absorbent surface (reaction 1), further carbonation is hindered. However, when certain water content is present, the dissolution of the layer of the just formed lithium carbonate takes place and the CO_2 capture is promoted again. In a different work, Ochoa-Fernández et al. have also reported the effects of water steam addition on the CO_2 capture, but in this case the experiments were performed at high temperatures [13]. They studied the effect of water vapor on the CO_2 capture and regeneration rates for several lithium ceramics sorbents including Li_4SiO_4, observing that water addition improves the kinetic of both, the CO_2 capture and ceramic regeneration processes. Authors suggest that this behavior could be attributed to a high mobility of the alkaline ions caused by the presence of water steam, which in fact, is one of the limiting factors of the CO_2 absorption process.

Based on the above, since the mechanisms involving the reaction between Li_4SiO_4 and H_2O seems to modify the CO_2 absorption, but the phenomenon is not well understood, the aim of this work was to systematically study the hydration process of Li_4SiO_4 and

---

* Corresponding author. Tel.: +52 55 5622 4627; fax: +52 55 5616 1371.
E-mail address: pfeiffer@iim.unam.mx (H. Pfeiffer).

to elucidate the different physicochemical events involved in this process.

2. Experimental

Lithium orthosilicate was synthesized by the technique of solid-state reaction using silicic acid (H_2SiO_3, J.T. Baker) and lithium carbonate (Li_2CO_3 99+% purity, Sigma–Aldrich) powders as starting materials. Reagents were mechanically mixed in a mortar, and in order to prevent the sublimation of lithium, the mixtures were prepared using a lithium excess of 5%, based on the stoichiometric lithium content on Li_4SiO_4. The resultant powders were heat-treated at 850 °C for 6 h in air, following a heating rate of 5 °C/min. After that, the sample was characterized by X-ray diffraction (XRD) and scanning electron microscopy (SEM). For the XRD characterization a diffractometer (Bruker AXS, D8 Advance) coupled to a copper anode X-ray tube was used. Compounds were identified by the corresponding Joint Committee Powder Diffraction Standards (JCPDS). Scanning electron microscopy micrographs were obtained in a Cambridge Leica Stereoscan 440 microscope. The sample was previously coated with gold to avoid the lack of electrical conductivity.

Once the sample was characterized, different dynamic water vapor sorption experiments were carried out in a temperature-controlled thermobalance TA Instruments model Q5000SA, where experimental variables were temperature, time and relative humidity (RH). The RH was automatically controlled by the Q5000SA thermobalance, using in all the cases N_2 (grade 4.8, from Praxair) as carrier gas with a flow of 100 ml/min. First, water vapor sorption/desorption isotherms were generated at different temperatures between 25 and 70 °C, varying the relative humidity from 10 to 85 and from 85 to 10% to form a cycle. Additionally, different adsorption curves were obtained maintaining the RH constant (20, 40, 60 and 80% RH), but varying the temperature from 25 to 75 °C. Finally, isothermal experiments were performed at different temperatures and RH values.

After the water sorption experiments, and in order to identify the hydration products, the samples were characterized by standard thermogravimetric (TG) and infrared (FTIR) analyses. These experiments were performed at environmental conditions. For the TG analyses, the experiments were performed with a heating rate of 3 °C/min into a thermobalance TA Instruments model Q500HR. For the FTIR spectroscopy, samples were prepared as KBr pellets and the analyses were performed on a Spectrometer NICOLET 6700 FT-IR.

3. Results and discussion

The diffraction pattern of the Li_4SiO_4 sample, produced by solid state reaction, shows the characteristic pattern of Li_4SiO_4 phase (Fig. 1A) according to the JCPDS file number 37-1472. Furthermore, the synthesized powders show a size distribution with high dispersion, where the particle sizes are between 50 and 70 μm (inset Fig. 1B).

The sorption/desorption isotherms of water vapor on Li_4SiO_4 are shown in Fig. 2. According to the IUPAC classification, the isotherms generated at 25 and 30 °C correspond to adsorption curves type II, while the adsorption isotherms measured in the range of 35–70 °C corresponded to type III. Isotherms types II are commonly observed in the case of nonporous adsorbents where the unrestricted monolayer–multilayer formation can take place. On the other hand, isotherms type III are commonly obtained in systems where the interactions between the adsorbate and the adsorbent are relatively weak but the adsorbate–adsorbate interactions are significant like in the case of water vapor adsorption [14].
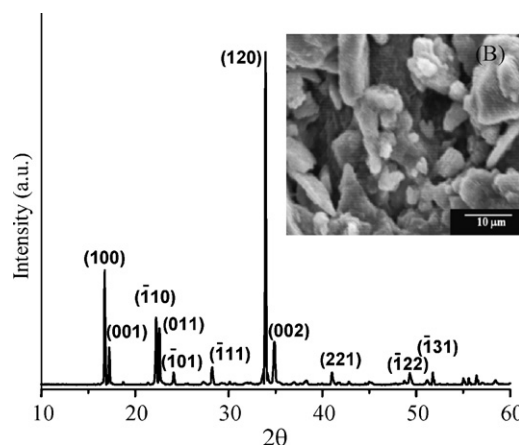

Fig. 1. Lithium orthosilicate (Li_4SiO_4) synthesized by solid stated reaction: (A) XRD pattern of the obtained phase and (B) SEM image showing the particle size and morphology.

Additionally, although all the isotherms present hysteresis loops, two different behaviors are observed. At temperatures lower than 45 °C, the hysteresis loops practically closed, this behavior suggest that adsorption/desorption process is reversible. In these cases, the maximum increment in mass is lower than 1% at RH values of 10% for the different temperatures after desiccation (Fig. 2A).

At temperatures equal to or higher than 45 °C, the isotherms presented a plateau during desorption (desiccation). The most evident plateaus are observed in the isotherms performed at 60 and 70 °C (Fig. 2B). In fact, in these curves the hysteresis loops did not close any more, and a final mass gains after desorption processes were registered. In these cases, the mass gain is up to 3%. These two different behaviors were explained by the presence of different processes, at these specific conditions not only water adsorption was carried out, but a chemical process could be present as well. Then it should be assumed that the process presented at temperatures lower than 45 °C is water adsorption over the surface of the Li_4SiO_4 particles and in these cases, the mass gained by the samples was only due to the increasing thickness of multilayer adsorbed films. On the other hand, in samples treated at 50 °C or higher temperatures, the results are indicative that in these cases not only a physical adsorption went through, but a chemical reaction took place, so an absorption process happened. It would be attributed to the formation of hydroxyl species over the surface of Li_4SiO_4 particles.

Besides, respect to the isotherms made at high temperatures (Fig. 2B), it should be mentioned two different loss of mass which were presented during desorption stage; the first one was presented between 82 and 77% RH, while the second one began at 34% RH. The first loss of mass can be explained as spontaneous evaporation of condensed water located at the particle surfaces, and the second process must correspond to evaporation of water located at inter-particle spaces when the equilibrium between adsorbed film and saturated vapor atmosphere in the system change and the adsorption process became reversible. Besides, in the isotherms performed at 60 and 70 °C a continuous mass increase is observed between the two desorption processes. It is an indicative that the absorption continued at these temperatures and RH conditions.

The existence of two sorption processes is supported by Fig. 3 where the maxima mass gain due to trapped water during the sorption are summarized for the different isotherms. At low temperatures, adsorption takes place which leads to a mass increase. At higher temperature, on the other hand, adsorption is hindered due to the temperature increase but chemical processes are promoted, then two behaviors are observed. Both sorption processes
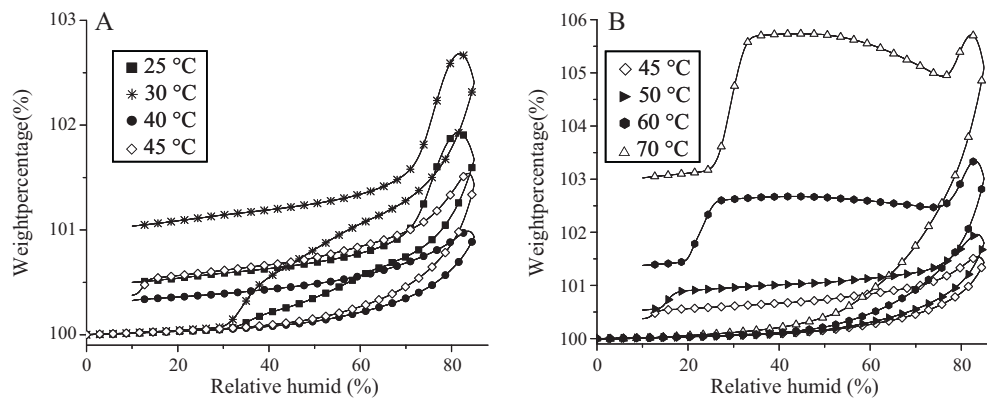
Fig. 2. Water adsorption/desorption isotherms on Li_4SiO_4 generated at different temperatures.

are taking place at the same time but a close inspection of Fig. 3 suggests that for temperatures equal to or higher than 50 °C absorption seems to be the dominant process while for temperatures equal or lower than 30 °C adsorption is dominating.

In order to analyze and confirm the presence of hydration products, two different analyses were performed; FTIR and TGA. All these experiments were carried out on the samples after their temperature-humidity treatments. FTIR data (Fig. 4) reveal the presence of absorption bands characteristic of silicon–oxygen bonds and lithium–oxygen bonds, as well as carbonate and hydroxyl species located over the surface of the Li_4SiO_4 particles [15–26]. All these bands could be classified into two groups: bands produced by vibrations from the bulk of the Li_4SiO_4 crystals, such as Si–O, Li–O bonds, or related, which did not present significant changes among the samples; and a second group of bands which were attributed to different species formed over the surface of the Li_4SiO_4 crystals, such as carbonate or hydroxyl species. The intensity of the second group of bands changed as a function of the temperature-humidity treatments, as it is shown in Fig. 4.

The absorption bands originated from Si–O– and Li–O– groups were located at 430, 476 and 980 cm^{-1} [15,18,22]. In addition, bands associated with vibrations of O–Si–O and Si–O–Si bridges occur at 795 and 828 cm^{-1}, respectively [15,18,20,22]. Bands at 732, 863, 1436 and 1477 cm^{-1} were attributed to Li_2CO_3 vibrations [15], while the band located at 952 cm^{-1} is due to the asym-

metric stretching vibrations of Si–OH silanol groups [16,19–21]. In general, FTIR results are in accordance with the formation of lithium and silicon hydroxide species over the surface of the Li_4SiO_4.

Moreover, an interesting aspect to be pointed out from the FTIR results is the fact that band vibrations of the terminal Si–O– and Li–O type bonds decreased in intensity, when the water content used during the absorption experiment was increased. On the other hand, the bands generated due to silicon hydroxyl groups grew in intensity, as a function of the water content, which indicates an increase in the number of superficial hydroxyls (Si–OH). These results strongly suggest that the reaction of atmospheric water vapor with Li_4SiO_4. It could be started on surface active sites of ceramic, where non-bonding ions are present; such as non-bonding oxygens (Si–O–) as well as lithium (Li–O–) with the subsequent formation of hydroxylated species on surface. Latter, the material carbonation is produced due to the contact between the environmental CO_2 and the hydroxylated surfaces. This process was evidenced by the increment of the bands at 732, 863, 1436 and 1477 cm^{-1} attributed to lithium carbonate on the samples treated at higher temperatures and relative humidity (Fig. 4). The above means that the formation of superficial lithium hydroxyls must play an important role on the atmospheric CO_2 absorption process,

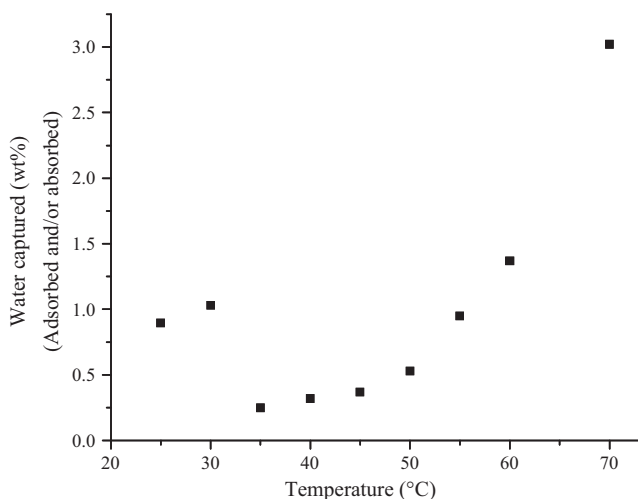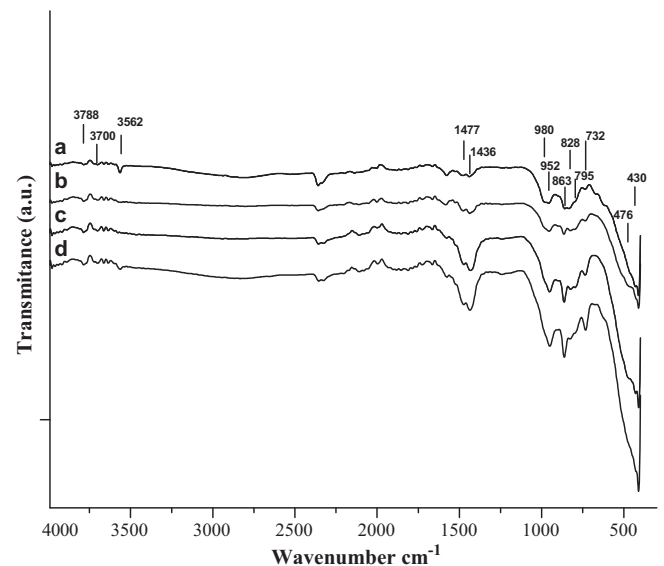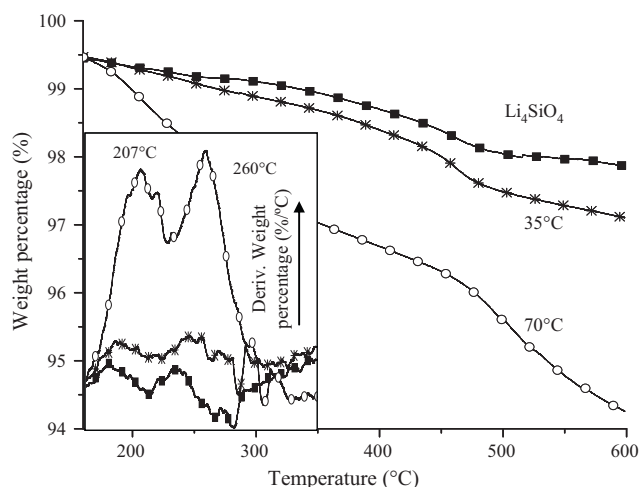**Fig. 3.** Total water captured after sorption–desorption cycles at different temperatures.

**Fig. 4.** Infrared spectra of the Li_4SiO_4 samples recorded after humidity treatment: (a) Li_4SiO_4 without any treatment, (b) heat treated at 35 °C, (c) at 60 °C and (d) and at 70 °C.

Fig. 5. TGA curves of the Li$_4$SiO$_4$ samples after humidity treatment: Li$_4$SiO$_4$ without any thermal treatment, sample previously treated at 35 °C and sample previously treated at 70 °C. The inset shows the derivative curve of thermogravimetric data for the three samples. All the samples were normalized in mass, after the water desorption, at 150 °C.

through the following process (reaction 2):

$$2LiOH_{(s)} + CO_{2(g)} \rightarrow Li_2CO_{3(s)} + H_2O_{(v)},$$
$$\Delta G = -97 \text{ kJ/mol at } 25 \, °C \tag{2}$$
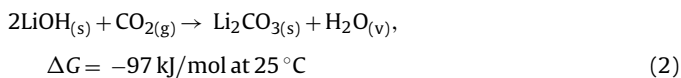
Two more bands at 3700 and 3788 (Fig. 4) correspond to different O–H vibrations, such as Si–OH and Li–OH [26]. However these bands do not change significantly as a function of the thermal treatment; a possible explanation is that Si–OH and Li–OH are consumed during the exposure of the humidified powder to air.

In addition, two samples previously temperature-humidity treated at 35 and 70 °C, as well as the Li$_4$SiO$_4$ original sample, were analyzed by TGA (Fig. 5). It is evident that although the three samples lost mass showing similar changes in the slopes, the quantity of mass loss varied importantly. Initially, for the sample temperature-humidity treated at 70 °C, two decrements of mass between 125 and 306 °C are observed. They are attributed to the thermal decomposition of lithium and silicon hydroxyl species, respectively. Based on bonding energy values for Li–OH (447 kJ/mol) and Si–OH (452 kJ/mol) [27], and on the derivative temperature curves (inset Fig. 5), it was assumed that 207 °C corresponds to the thermal decomposition of lithium hydroxyl groups. Therefore, the process at 260 °C should correspond to the thermal decomposition of the silanols groups. The mass loss at higher temperatures could be attributed to different decarbonation processes. The same processes seem to occur in all the samples including the untreated Li$_4$SiO$_4$ sample. The amount of mass loss should be proportional to the concentrations of carbonate and hydroxyl species formed during the temperature-humidity treatments. It implies that even the untreated Li$_4$SiO$_4$ sample already possess some hydroxyl groups over the surface of the particles. It has to be assumed that these hydroxyl and carbonate species were produced due to the contact of these particles with the atmospheric water vapor and CO$_2$.

Once the different processes between the Li$_4$SiO$_4$ and water vapor were identified and characterized, a different set of experiments were perform in order to obtain some extra information. In this case (Fig. 6), the change in mass was monitored as a function of the sample temperature while in the atmosphere, a given level of humidity was established (20, 40, 60 and 80% RH). In these curves, two different processes are evident: (1) at very low temperatures the mass shows different increments, which could
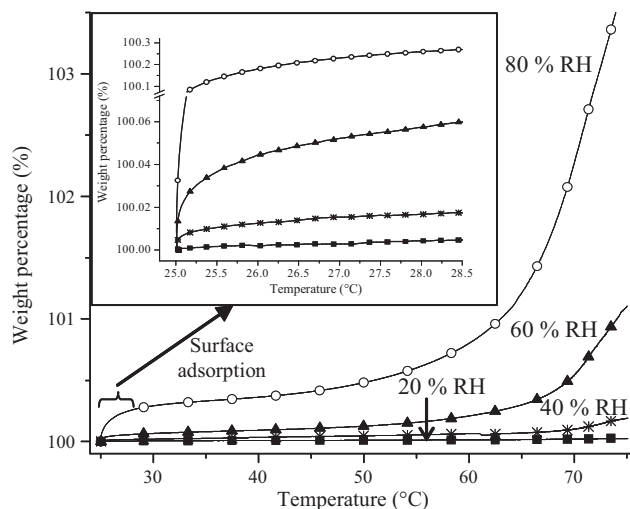
Fig. 6. Water absorbed by Li$_4$SiO$_4$ particles in a dynamic process at different relative humid (RH) conditions.

be attributed to water adsorption on the Li$_4$SiO$_4$ surface (inset Fig. 6). It is also possible to observe in Fig. 6, that the amount of water adsorbed is function of the RH present in the atmosphere, as expected. The mass of adsorbed water increased from 0.01% at a RH of 20%, to 0.27% at a RH equal to 80%, as soon as the experiments began (temperature <30 °C). (2) Latter, when the temperature was increased the second process was evidenced. The second increment of mass must be associated to water absorption, in other words, to the Li–OH and Si–OH superficial formation. Although the quantity of water absorbed increases gradually as a function of the RH and temperature, it may be defined an approximated temperature in which the H$_2$O absorption is activated by calculating the inflection points. Table 1 presents the mass gained in each RH level, at the maximum temperature of the experiment (75 °C), and the temperature corresponding to the inflection points, where absorption process seems to be activated for each RH. As expected, the higher the water concentration in the atmosphere the smaller the onset temperature necessary to activate the absorption.

In order to further understand the water vapor absorption mechanisms on Li$_4$SiO$_4$, different isothermal experiments were carried out at 55, 60, 65 and 70 °C and RH values equal to 60, 65, 70 and 75%. Fig. 7 shows the different isotherms obtained, where in general the four sets of samples behave in a similar way. All these isotherms can be divided on two different periods of time: in the first seconds, as it could be expected, the phenomenon occurring must be the water adsorption. Nevertheless, in this period of time the equipment presents a dead time of several seconds, corresponding to the time where the RH increases from zero to the set value of RH. Hence, this information could not be accurate. On the other hand, at long times all the isotherms were, initially, fitted to a double exponential model, assuming that water absorption took place, but water adsorption could happen as well. However, the two rate constants tend to converge

Table 1
Maximum water absorbed at 75 °C and absorption activation temperatures (inflection points in Fig. 6) at the different relative humidity (RH) values.

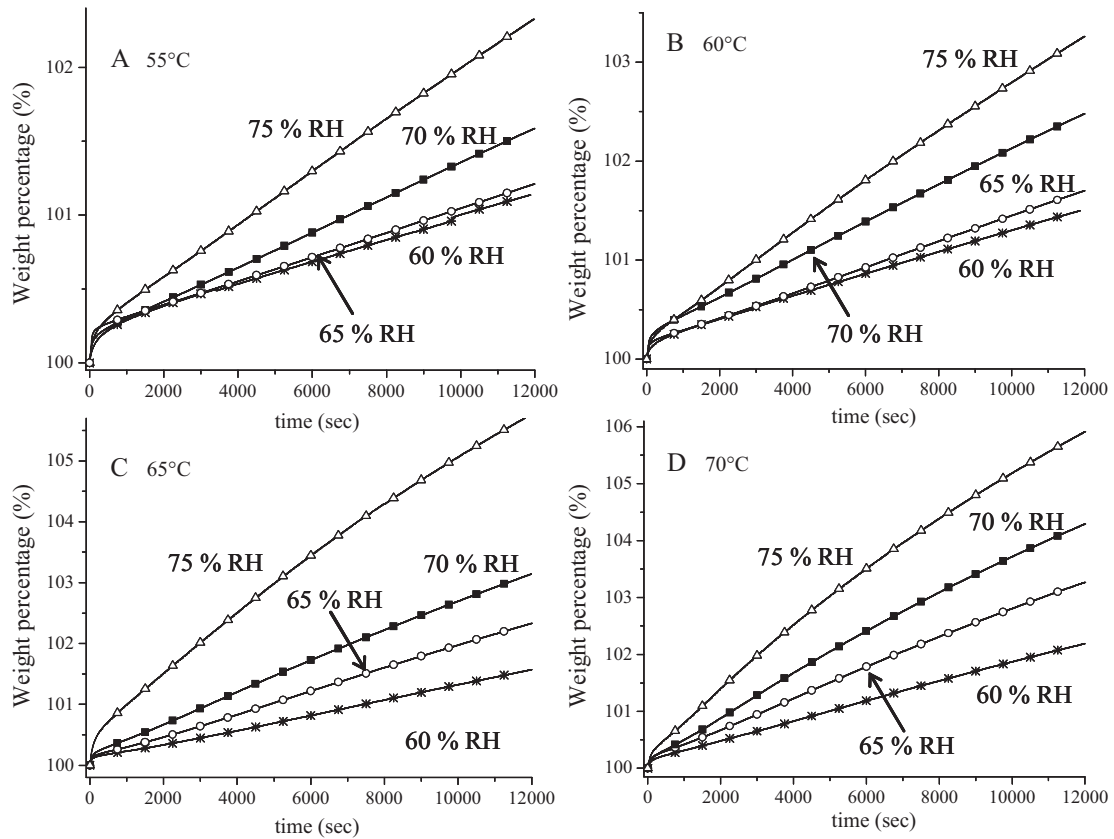| RH (%)	Water gain at 75 °C (%)	Absorption onset temperature (°C)
80	3.92	63
60	1.12	68
40	0.19	71
20	0.02	71

Fig. 7. Isotherms obtained at different RH levels and at different temperatures: (A) 55 °C, (B) 60 °C, (C) 65 °C and (D) 70 °C.

to the same value, which suggests that only one process occurs at long times. This process must correspond to water absorption, as water adsorption was initially produced and it may have reached the equilibrium. Therefore, a single exponential model can be used to determine the water absorption rate constant value (k):

$$W = A \exp^{-kt} + C \tag{3}$$

Here W is the captured water; A and C are the pre-exponential and the y-intercept values; k is the kinetic constants and t is the time.
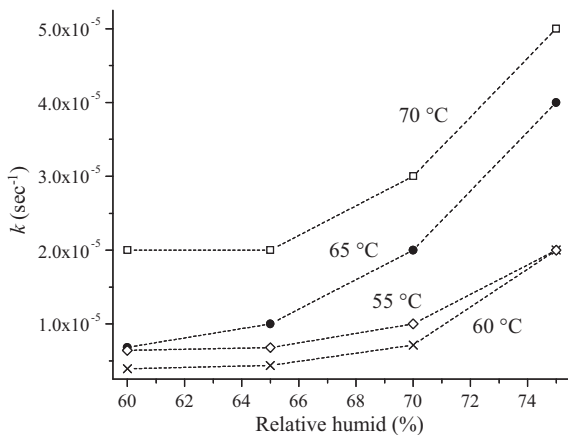

Fig. 8. Rate constants (k) calculated from the equation 3 as a function of the RH at different temperatures.

Fig. 8 plots the different k values as a function of the relative humidity. In general, it can be seen that k values increase as a function of the RH and the temperature. Therefore, the water absorption on Li_4SiO_4 is faster when the temperature and/or the RH are increased. Nevertheless, the curve corresponding to 55 °C presents higher k values than the curve at 60 °C. The rate constant k, calculated for curves at 55 °C is actually dominated not only by absorption but by adsorption too. However, the mass gained at this temperature is always lower than that obtained at 60 °C (Fig. 7A and B). This result fits well with the estimated activation temperatures for absorption (Table 1).

Finally, to analyze the temperature dependence of water absorption under different RH, the Eyring's model was used [28]:

$$\ln\left(\frac{k}{T}\right) = -\left(\frac{\Delta H^{\ddagger}}{R}\right)\left(\frac{1}{T}\right) + \ln E + \frac{\Delta S^{\ddagger}}{R} \tag{4}$$

where k is the rate constant value of the water absorption process; E represents a pre-exponential factor, which in Eyring's formulation is equal to the ratio of Boltzmann's constant to Planck's constant; $\Delta H^{\ddagger}$ and $\Delta S^{\ddagger}$ are the activation enthalpy and entropy, respectively.

The effect of temperature on the rate constants of the water absorption process, on Li_4SiO_4 is illustrated in Fig. 9. It is clear that plots of $\ln(k/T)$ versus $1/T$ describe linear trends, fitting to the model. Therefore, fitting the data to linear plots gave the activation enthalpies ($\Delta H^{\ddagger}$) for the water absorption processes on Li_4SiO_4 at different RH. It has to be mentioned that, based on the results and interpretation obtained previously for the data at 55 °C, these values were not included into the $\Delta H^{\ddagger}$ calculation at low temperatures. $\Delta H^{\ddagger}$ values for the water absorption process decrease due to the RH increment. The $\Delta H^{\ddagger}$ values obtained varied from 5528.6 J/mol to 2074.2 J/mol at 60% and 75% RH, respectively. The
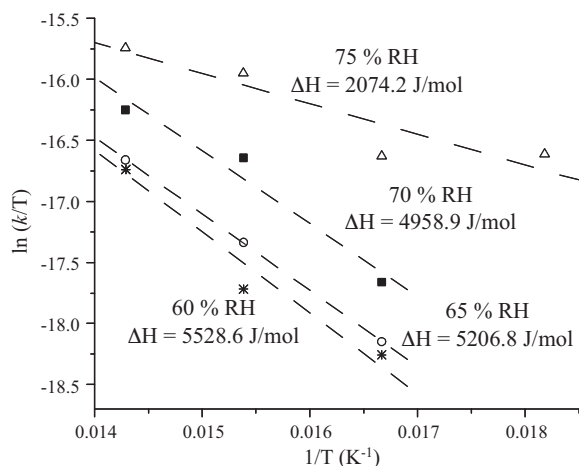
Fig. 9. Eyring's plots for the rate constants (k) of water absorption at different RH.

$\Delta H^{\ddagger}$ decreased 62.5% by the increment of RH. This result clearly shows that water vapor concentration plays a very important role on the reactivity with Li_4SiO_4, which may affect on different manners the CO_2 absorption on this or any other lithium ceramic.

4. Conclusions

Summarizing, it was observed that Li_4SiO_4 is able to trap water by two different mechanisms; adsorption and absorption. The characteristics of any of these sorption processes depend on different factors such as temperature and humid relative concentration. Therefore, the stability and/or chemical reactivity of Li_4SiO_4 must be altered by the presence of water. Additionally, these phenomena must occur not only at temperatures lower than 100 °C but at higher temperatures, where different hydroxyls (Li–OH and Si–OH) may be instantaneously produced.

In addition, the kinetic analysis confirms the importance of temperature and RH during the water adsorption and absorption. Additionally the rate constants for water absorption were determined. It was found that the absorption process experimentally determined during this work, follows the behavior described by the Eyring's model so, the activation enthalpies ($\Delta H^{\ddagger}$) for the water absorption process were calculated. $\Delta H^{\ddagger}$ values decreased while the RH is incremented. These values range from 5528.6 J/mol at 60% of RH to 2074.2 J/mol at 75% RH. These results clearly show that water vapor concentration is an important factor on the Li_4SiO_4 stability, and it may affect the CO_2 absorption of this ceramic. All this information should be taken into account during the analyses of lithium ceramics for different applications, where the presence of water may be a component of the entire system.

References

[1] D. Cruz, S. Bulbulian, E. Lima, H. Pfeiffer, J. Solid State Chem. 179 (2006) 909–916.
[2] C.E. Johnson, J. Nucl. Mater. 270 (1999) 212–220.
[3] C.E. Johnson, R.G. Clemmer, G.W. Hollenberg, J. Nucl. Mater. 103 (1981) 547–553.
[4] H. Pfeiffer, P. Bosch, B. Bulbulian, J. Nucl. Mater. 257 (1998) 309–317.
[5] Y. Chikhray, V. Shestakov, O. Maksimkin, L. Turubarova, I. Osipov, T. Kulsartov, A. Kuykabayeba, I. Tazhibayeva, H. Kawamura, K. Tsuchiya, J. Nucl. Mater. 386–388 (2009) 286–289.
[6] M.J. Venegas, E. Fregoso-Israel, R. Escamilla, H. Pfeiffer, Ind. Eng. Chem. Res. 46 (2007) 2407–2412.
[7] H. Pfeiffer, Advances in CO_2 Conversion and Utilization; Chapter 15: Advances on alkaline ceramics as possible CO_2 captors, ACS Series Books, 1056 (2010) 233–253.
[8] M. Kato, Y. Maezawa, S. Takeda, Y. Hagiwara, R. Kogo, K. Semba, M. Hamamura, Key Eng. Mater. 317–318 (2006) 81–84.
[9] B.N. Nair, R.P. Burwood, V.J. Goh, K. Nakagawa, T. Yamaguchi, Prog. Mater. Sci. 54 (2009) 511–541.
[10] N. Roux, S. Tanaka, C. Johnson, R. Verrall, Fusion Eng. Des. 41 (1998) 31–38.
[11] J.D. Figueroa, T. Fout, S. Plasynski, H. Macllvried, R.D. Srivastava, Inter. J. Greenhouse Gas Control 2 (2008) 9–20.
[12] K. Essaki, K. Nakagawa, M. Kato, H. Uemoto, J. Chem. Eng. Jpn. 37 (2004) 772–777.
[13] E. Ochoa-Fernández, T. Zhao, M. Ronning, ChenF D., J. Environ. Eng. 135 (2009) 397–403.
[14] S. Lowell, J.E. Shields, M.A. Thomas, Characterization of porous solids and powders: surface area, pore size an density, in: Particle Technology Series, Kluwer Academic Publishers, London, 2004.
[15] B. Zhang, M. Nieuwoudt, A.J. Easteal, J. Am. Ceram. Soc. 91 (2008) 1927–1932.
[16] J. Yan, S. Shih, K. Jung, D.L. Kwong, M. Kovar, J.M. White, B.E. Gnade, L. Magel, Appl. Phys. Lett. 64 (1994) 1374–1379.
[17] G.D. Chukin, V.I. Malevich, J. Appl. Spectrosc. 26 (1977) 223–229.
[18] R. Ravikrishna, R. Green, K.T. Valsaraj, J. Sol–Gel Sci. Technol. 34 (2005) 111–122.
[19] R. Soda, Bull. Chem. Soc. Jpn. 35 (1962) 1897–1898.
[20] W. Geng, R. Wang, X. Li, Y. Zou, T. Zhang, J. Tu, Y. He, Li.F N., Sens. Actuat. B 127 (2007) 323–329.
[21] C.T. Wang, C.L. Wu., Thin Solid Films 496 (2006) 658–664.
[22] F. del-Monte, W. Larsen, J.D. Mackenzie, J. Am. Ceram. Soc. 83 (2000) 628–634.
[23] K. Hermansson, G. Gajewski, P.D. Mitev, J. Phys. Chem. A 112 (2008) 13487–13494.
[24] Y. Hee-Sun, C. Se-Young, H. Sang-Hoon, P. Chan-Gyung, Thin Solid Films 348 (1999) 69–73.
[25] J.P. Gallas, J.M. Goupil, A. Vimont, J.C. Lavalley, B. Gil, J.P. Gilson, O. Miserque, Langmuir 25 (2009) 5825–5834.
[26] V.C. Farmer, The Infrared Spectra of Minerals, Mineralogical Soc. Monographs, Mineral. Soc. Press, 1977.
[27] J.E. Huheey, Inorganic Chemistry. Principles of structure and reactivity, second edition, Harper and Row Publishers, New York, 1978.
[28] K.J. Laidler, M.C. King, J. Phys. Chem. 87 (1983) 2657–2664.